Tellus (2004), 56B, 105–117
Printed in UK. All rights reserved

TELLUS

Eddy correlation measurements of aerosol deposition to grass

By RICHARD J. VONG[1]*, DEAN VICKERS[1] and DAVID S. COVERT[2], [1]*College of Oceanic and Atmospheric Sciences, Oregon State University, Corvallis, OR, 97331-5503, USA;* [2]*Department of Atmospheric Sciences, University of Washington, Seattle, WA 98195, USA*

(Manuscript received 2 January 2003; in final form 4 December 2003)

ABSTRACT

An experiment was conducted to measure aerosol turbulent fluxes to a grass field. A new high-flow-rate aerosol sensor was deployed from a tower to make eddy correlation (EC) measurements of aerosol turbulent flux and deposition velocity. The EC data were screened and analysed for uncertainties associated with advection, boundary layer growth, instrument separation and counting particles. An apparent bias in the aerosol flux due to particle hygroscopic growth was evaluated from chemical and microphysical measurements and removed from the results based on derived corrections. The resulting aerosol deposition velocity for 0.52 μm diameter particles depended on atmospheric stability with values of 0.3 cm s^{-1} during near-neutral stability, 0.44 cm s^{-1} during unstable periods and 0.16 cm s^{-1} during stable periods with an estimated uncertainty of $\pm$0.07 cm s^{-1} due to chemical composition and particle counting.

1. Introduction

Aerosol turbulent flux and dry deposition have been difficult to measure and interpret because a large number of controlling and confounding factors can contribute to observed fluxes. These factors include effects that are related to boundary layer dynamics and aerosol microphysics as well as limitations in the flux measurement technique.

Aerosol deposition is influenced by particle, vegetation and atmospheric boundary layer characteristics. Particles with diameters between 0.1 and 1 μm are typically removed by impaction and interception onto the fine structural elements of vegetation after transport by turbulent eddies. Aerosol flux measurements also are influenced by horizontal advection of aerosol emitted by upwind sources (Slinn, 1983) and entrainment of air from aloft (Businger, 1986); these processes can result in a vertical divergence of the aerosol flux such that deposition to the underlying surface is not equivalent to the flux at the measurement height (section 1.1). Aerosol concentration (for particles in a fixed diameter interval) is not typically a conservative property in that many particles undergo hygroscopic growth, or shrinkage, during transport through the boundary layer; this process can produce fluxes (Fairall, 1984; Businger, 1986) that depend on humidity (section 1.2) as much as on particle transport by turbulence. The eddy correlation (EC) technique for measuring fluxes has uncertainties that depend on the number of particles counted; these counting errors can be large when commercial instrumentation is used (Fairall, 1984).

Here we describe simultaneous observations of aerosol fluxes that were obtained using the EC micrometeorological technique. The factors influencing measured aerosol deposition to the underlying grass field were addressed by: (a) deploying a new high-flow-rate optical instrument to increase particle counting rate, (b) locating the field site in flat terrain and away from upwind emission sources to minimize advection, (c) utilizing data selection criteria to avoid time periods with advection or boundary layer growth, (d) measuring aerosol chemical and microphysical properties, (e) measuring heat and vapour fluxes and (f) deriving and applying corrections to quantify the effect of hygroscopic growth on the observed aerosol flux.

It is convenient and useful to describe aerosol turbulent flux in terms of an aerosol turbulent deposition velocity

$$V_{\mathrm{dt}} = \overline{w'N'}/\overline{N} \tag{1}$$

where $\overline{N}$ is the 30 min mean aerosol number concentration within a fixed diameter interval (in particles cm^{-3}) (note that all "overbars" denote mean quantities, usually over 30 min); N' is the instantaneous deviation of a 10 Hz measurement from mean aerosol number concentration (all primed variables are 10 Hz deviations from the mean); w' is the instantaneous deviation of the vertical wind velocity from its mean ($\overline{w}$; positive values for $\overline{w}$ and w' are directed upwards, away from the surface); and $\overline{w'N'}$ is the assembly average vertical velocity–aerosol number

*Corresponding author.
e-mail: vong@coas.oregonstate.edu

concentration covariance within a fixed diameter interval, i.e. the EC aerosol turbulent flux.

V_{dt} can be thought of as a 'mean-scaled' turbulent flux and also can be calculated in terms of aerosol mass or spectral density in eq. (1). The aerosol size distribution is often described using a power law (Junge, 1963) where the number concentration of particles (in some diameter interval ΔD, i.e. aerosol spectral density $\mathrm{d}N/\mathrm{d}D$) is related to the mean diameter (D) in the interval as

$$\mathcal{N} = \mathrm{d}N/\mathrm{d}D = cD^{-(\beta+1)} \tag{2}$$

where β is the Junge power-law exponent and c is a site-specific constant.

In this study we use β to relate measurements of aerosol number concentration at two adjacent diameters because it is analytically convenient (see Appendix A). While this power law does not characterize the aerosol number–size distribution well over a large size range, it is applicable to the limited size ranges considered in this study (e.g. using four separate values of β, one for each aerosol flux, for portions in the interval: 0.3 μm < diameter < 1.0 μm; see Table 3).

Hygroscopic growth and shrinkage of atmospheric aerosol will affect particle diameter and, thus, measurements of their behavior in the turbulent boundary layer. Water-soluble aerosol particles swell to approximately twice their "dry" diameter as relative humidity (RH) increases to 90%; this "hygroscopic growth" phenomenon is fast enough (Keith and Arons, 1954) that most particle sizes may be considered to be nearly in equilibrium with the local RH (Fairall, 1984). Swietlicki et al. (2000) used empirical expressions to characterize the hygroscopic behaviour of atmospheric aerosol particles on the basis of parameters that are measured directly for ambient aerosol or modelled for specific chemical compositions. This relationship between the particle diameter at ambient water vapour saturation ratio $D(S)$ and the dry diameter D_0 is

$$D(S)/D_0 = (1 - S)^{-\gamma} \tag{3}$$

where γ is a hygroscopic growth parameter that depends on chemical composition and S is the water vapour saturation ratio ($S = \mathrm{RH}/100\%$).

Experimental data (Swietlicki et al., 2000) suggested a value for γ of 0.214 for "aged European air" of mixed continental–anthropogenic origin with larger values for γ when marine aerosols were characterized.

1.1. Budget equation for aerosol turbulent fluxes

In order that aerosol flux measured from a tower will also describe aerosol deposition to an underlying vegetated surface (i.e. $\overline{w'N'}$ is constant with height), the conservation equation (Stull, 1988) states that aerosol advection and time change (also termed "storage") must either be absent or that these terms must cancel. Equation (4) presents the 2-D balance between the time change (term 1 on the left-hand side (l.h.s.)), horizontal streamwise advection (term 2 on the l.h.s.), and vertical divergence of the turbulent flux (term 4 on the l.h.s.) that occurs when streamwise turbulent diffusion (term 3 on the l.h.s.), Brownian diffusion (term 1 on the r.h.s.), divergence of gravitational settling (term 2 on the r.h.s.) and aerosol sources (S) are all negligible or in balance:

$$\partial\overline{N}/\partial t + \partial(\overline{u}\overline{N})/\partial x + \partial(\overline{u'N'})/\partial x + \partial(\overline{w'N'})/\partial z = D(\partial^2\overline{N}/\partial z^2) - \partial(v_g\overline{N})/\partial z + S. \tag{4}$$

In this equation $\overline{N}$ is mean aerosol number concentration in a specific, fixed, diameter interval, u is wind speed along the streamwise horizontal direction, v_g is sedimentation velocity, D is the particle Brownian diffusion coefficient for a particular diameter, S is any *in situ* source of aerosol (coagulation, nucleation, emission), x is the streamwise horizontal coordinate, and z is the vertical coordinate (in a rotated coordinate system; see below and section 3).

Equation (4) illustrates why one would not estimate surface deposition for time periods when an aerosol source was located upwind (horizontal advection) or when aerosol concentration is changing substantially (time change, i.e. "non-stationarity") because vertical divergence in the aerosol flux is likely. Unfortunately, these conditions frequently occur such that many EC studies of aerosol flux will not provide quantitative estimates of deposition to terrestrial ecosystems unless the impacts of terms 1 and 2 cancel (Slinn, 1983; Businger, 1986). In the absence of vertical flux divergence, the measured turbulent flux is the aerosol deposition to the underlying surface.

1.2. Effect of heat and vapour fluxes on aerosol turbulent flux

Turbulent heat and vapour vertical fluxes introduce a net mass, or density, flux for a scalar even when the vertical velocity is zero for the averaging period. This correction (Webb et al., 1980) accounts for the differences between an appropriate assumption that there is no net mass flux of air into the ground and its usual application as, instead, assuming a zero mean vertical velocity during any flux averaging period (30 min here). These two assumptions are equivalent only when there is no heat or vapour flux because density will vary with height due to temperature and/or vapour gradients. The Webb, or density flux, correction (Businger, 1986) is in the form of a calculated vertical velocity ($\overline{w}$), that is

$$\overline{w} = 1.61(\overline{w'\rho_{\mathrm{H2O}'}}/\rho_{\mathrm{air}})(1 + 1.61q)(\overline{w'T'}/T) \tag{5}$$

where ρ_{H2O} is the density of water vapour, ρ_{air} is the density of dry air, q is the specific humidity $= \rho_{\mathrm{H2O}}/\rho_{\mathrm{air}}$, T is the mean ambient air temperature, 1.61 is the ratio of molecular weights of dry air and water vapour, $\overline{w'T'}$ is the assembly average kinematic turbulent heat flux measured by EC, $\overline{w'\rho_{\mathrm{H20}'}}$ is the assembly average water vapour turbulent flux measured by EC and $\overline{w}$ is the net 30-min vertical velocity that is needed to compensate for

the density flux (coordinate rotations to EC covariances set any other $\overline{w}$ to zero).

This 'density flux correction' is usually introduced (Hummelshoj, 1994) as a second term in the flux equation:

$$\overline{F} = \overline{w'N'} + \overline{w}\overline{N}. \quad (6)$$

The calculated mean vertical velocity ($\overline{w}$) is analogous to a second component of aerosol flux (term 2 on the r.h.s. of eq. (6)) that is added to that (term 1 on the r.h.s.) which was determined by EC. This density correction applies to any turbulent flux.

Hygroscopic growth represents a second dependence of aerosol flux on heat and vapour fluxes beyond the density correction (above). A saturation ratio turbulent flux is defined to help account for the change in the state of hydration of the aerosol as it is transported through an S gradient by near-surface turbulence (Fairall, 1984; Buzorius et al., 2000; Kowalski, 2001) as

$$\overline{w'S'} = \overline{w'q'}/q_{\text{sat}} - \overline{w'T'}(SL_{\text{v}})\Big/\left(R_{\text{v}}T^2\right) \quad (7)$$

where q_{sat} is the mean saturation value of the specific humidity, S is the mean ambient air saturation ratio (q/q_{sat}), $\overline{w'q'}$ is the water vapour turbulent flux (vertical velocity–specific humidity covariance), L_{v} is the latent heat of vaporization of water and R_{v} is the gas law constant for water vapour.

Corrections to aerosol turbulent fluxes for hygroscopic growth of particles are necessary when aerosol size at ambient RH is used to define N and, thus, the eddy flux. Previous derivations of these corrections by Fairall (1984) and Kowalski (2001) have been modified here (see Appendix A) to incorporate the Swietlicki et al. (2000) hygroscopic growth factor, γ, which is more easily measured in the field or estimated from lab data than is their empirical factor (K_f). Equation (8) provides an appropriate correction (ΔV_{d}) to the aerosol deposition velocity that is proportional to the exponent of the aerosol power-law size distribution (β), the humidity growth factor (γ) and the saturation ratio flux ($\overline{w'S'}$) but the correction is inversely proportional to the saturation ratio deficit ($1 - S$):

$$\Delta V_{\text{dt}} = -\beta\gamma\overline{w'S'}/(1 - S). \quad (8)$$

Upward saturation ratio fluxes ($\overline{w'S'} > 0$ are typical of wet soils underlying drier air) induce an apparent upward component to the aerosol flux and deposition velocity. This humidity correction produces a more downward aerosol flux (more negative) than is directly observed by EC measurements (the correction has the opposite sign from $\overline{w'S'}$ for the usual case where $\beta > 0$). In the absence of any surface removal of particles, eq. (8) states that an EC system based on aerosol concentration at ambient RH would observe an apparent (false) value of V_{dt} that is equal to the quantity $\beta\gamma\overline{w'S'}/(1 - S)$.

2. Experimental

The eddy flux and aerosol transport experiment (EFLAT) was conducted at a rural site located near Shedd, Oregon (24 km South of Corvallis, Oregon). Field measurements were made at 5 m above ground level (agl) from towers that were located in a flat, uniform field of rye grass; the 2 km (minimum) upwind fetch was "ideal" for performing micrometeorological measurements. The grass was 0.75 to 1 m tall during the EFLAT measurement period from 16 May to 15 June 2000.

Measurements of winds, aerosol concentrations and turbulent fluxes and momentum, heat and water vapour turbulent fluxes were performed utilizing open-path instrumentation mounted on a thin, triangular tower. Winds and virtual temperature were measured using a sonic anemometer (ATI SWS 211-3K) that did online averaging of 100 Hz transit-time observations to produce 10 Hz serial (RS-232) output data. Field measurements of aerosol concentration and diameter were performed at 15 min intervals using two commercial optical particle counting instruments (LASX and HSLAS, Particle Measurement Systems, Boulder, CO) and at 10 Hz by a new optical particle counting instrument (FAST, Droplet Measurement Technologies, Boulder, CO) that counted individual particles. Water vapour density was measured at 10 Hz with a UV absorption hygrometer (KH20, Campbell Sci., Ogden, UT). The three instruments were oriented into the prevailing wind direction by a boom extending ~1 m upwind of the tower. The lateral separation distances between the anemometer and the aerosol and water vapour instruments were 0.51 and 0.33 m respectively. There was no vertical or streamwise horizontal separation between these instruments (i.e. no lag time between scalar and wind measurements).

The hygrometer's voltage output was incorporated into the FAST aerosol spectrometer's RS-422 serial data stream after conversion to a digital signal. Instrument data processing and electronic delay times were accounted for in Visual Basic software running on a laptop computer with Windows NT. This "EC" logging system polled the aerosol spectrometer and hygrometer, calculated covariances and mean quantities, displayed real-time aerosol size distributions and produced output files consisting of synchronized 10 Hz raw data and 30-min means, variances and covariances. Four additional systems logged 15- to 30-min data (two Campbell 10x; two PCs) consisting of wind, T and RH vertical profiles, net radiation, soil heat flux and two aerosol instruments (LASX and HSLAS).

The FAST achieved a larger sensing volume per unit time (6.88 $\text{cm}^3\ \text{s}^{-1}$) than previously available instruments due to its high flow rate (80 m s^{-1}). Ambient air was pulled isokinetically (inlet cone diameter matched to wind speed) by an external pump through a 2 cm diameter test section. The residence time of the particles in the inlet and test section was ~1 ms. The FAST's laser ($\lambda = 680$ nm, 0.87 mm × 100 μm depth of field) passed through two sapphire windows and the aspirated aerosol before detection of the forward (5–14°) scattered light by masked and signal detectors. The instrument electronics determined which particles were located in the depth of field using the masked detector output, corrected the detector signal for baseline voltage and sorted the result into 20 software-selected size intervals. The FAST measured aerosol size at ambient T and RH. Aerosol

concentrations as a function of calibrated diameter (0.31 μm < diameter < 1.5 μm) were determined from particle counts and air volume (measured internally using a pitot tube and pressure transducers). There was no instrument dead time for the FAST; every particle was counted in real time and the concentrations were measured and output at a true 10 Hz data rate.

The size calibrations of the three aerosol field instruments were performed prior to EFLAT by generating aerosol in the laboratory and passing size-selected, monodisperse particles from a differential mobility analyser (DMA model 3071, TSI St Paul, MN) to the FAST, LASX and HSLAS through a small wind tunnel. Quadratic expressions related the responses of the three field instruments to calibration particles to the mobility-based Stokes diameter reported by the DMA for a $(NH_4)_2SO_4$ calibration aerosol. Comparisons performed before and after EFLAT showed no change in the FAST size calibration. Comparison of the FAST with a fourth light scattering instrument (PMS PCASP-100) showed that the FAST counting efficiency was 100% for particles with diameters greater than 0.375 μm but decreased as the diameter approached 0.31 μm; the FAST number concentrations for diameters <0.375 μm have been corrected for counting efficiency based on this intercomparison with the PCASP.

Impactor–filter sampling for aerosol chemical composition was performed at 1- to 3-day intervals throughout EFLAT. Ambient air was drawn from 5 m agl at 10 l min^{-1} through each of two sampling lines that consisted of an inertial impactor, sample filter, pump and dry gas meter. Filter changing and handling took place under clean conditions in a glove-box. After field collection, 38 Teflon filters were extracted ultrasonically in deionized water and methanol before chemical analysis for soluble ions (Na^+, Ca^{2+}, NH_4^+, SO_4^{2-}, and Cl^-) using ion chromatography. Eighteen quartz filters were analysed directly for total organic carbon and elemental carbon using a thermal-optical technique (Birch and Cary, 1996).

3. Data analysis methods

The 10 Hz tower data were used to calculate eddy fluxes as the covariance between each scalar (aerosol concentration in a selected diameter interval, water vapour density, temperature) and the vertical wind velocity. Data screening and quality assurance (Vickers and Mahrt, 1997) were utilized to identify periods with spikes, wind flow through the tower or equipment problems; these data were not used in subsequent analyses. Turbulent fluxes were calculated from 5-min (stable) or 10-min (unstable) mean quantities and then block averaged to 30-min values to reduce low-frequency contributions to the covariances. The use of the stability-dependent averaging timescale minimizes the influence of mesoscale motions on the calculated fluxes (Vickers and Mahrt, 2003). In order to obtain streamwise and vertical wind components, coordinate system rotations were performed to get a zero mean transverse and vertical velocity based the vertical attack angles determined using all data for a particular wind direction (Kaimal and Finnigan, 1994; Kowalski et al., 1997).

The hygrometer's output was drift-corrected by reference to co-located temperature and capacitance RH sensors (R. M Young HMP 45C) which had been extensively intercompared in the field. The temperature for heat fluxes was determined by correcting the sonic anemometer virtual temperature for specific humidity.

The 20 diameter intervals of the FAST aerosol spectrometer were reduced to four in the data analysis in order to maximize the total number of particles counted in a particular size interval to improve particle counting statistics. The FAST data thus constituted four scalar concentrations that subsequently were used in EC calculations of the aerosol turbulent fluxes. There is one FAST aerosol number concentration for each of the following size ranges:

(a) 0.31 < diameter < 0.375 μm,
(b) 0.375 < diameter < 0.716 μm,
(c) 0.716 < diameter < 0.98 μm, and
(d) 0.98 < diameter < 2.3 μm.

The geometric mean diameters for these four FAST size intervals, and the aerosol eddy fluxes, were 0.34, 0.52, 0.84 and 1.5 μm (Stokes diameter based on the $(NH_4)_2SO_4$ calibration).

The four FAST aerosol concentrations were each combined with rotated, vertical velocity for the calculation of aerosol eddy fluxes (Vong and Kowalski, 1995; Kowalski et al., 1997). These rotated aerosol fluxes are termed "uncorrected" herein. Subsequently, the 30-min aerosol eddy fluxes (as deposition velocities) were corrected for density (using eqs. (5) and (6)) and hygroscopic growth (using eqs. (7) and (8)) based on simultaneously measured values for the heat flux, vapour flux and the local slope (see Table 3) of the aerosol size distribution (β).

Data used to determine the final aerosol deposition velocities (Figs. 8 and 9) were stratified according to wind direction to separate periods with the best micrometeorological fetch ($260^\circ < \theta < 360^\circ$) from wind directions that brought recent pulp mill emissions to the sampling site ($90^\circ < \theta < 240^\circ$). In addition, data were screened to avoid both the morning transition period (6 to 10 a.m.) and near-saturated conditions (RH > 96%) because these conditions were not considered appropriate for determining aerosol turbulent flux to the surface. Near-saturated conditions were eliminated because they were not well described by the equation for hygroscopic growth and because gravitational sedimentation became significant (thus term 2 on r.h.s. of eq. (4) could become important) during these low-wind early morning periods.

4. Results and discussion

4.1. Meteorology

Clear or partly cloudy conditions were typical during EFLAT, although measurable (0.1–1 cm) precipitation occurred on 10

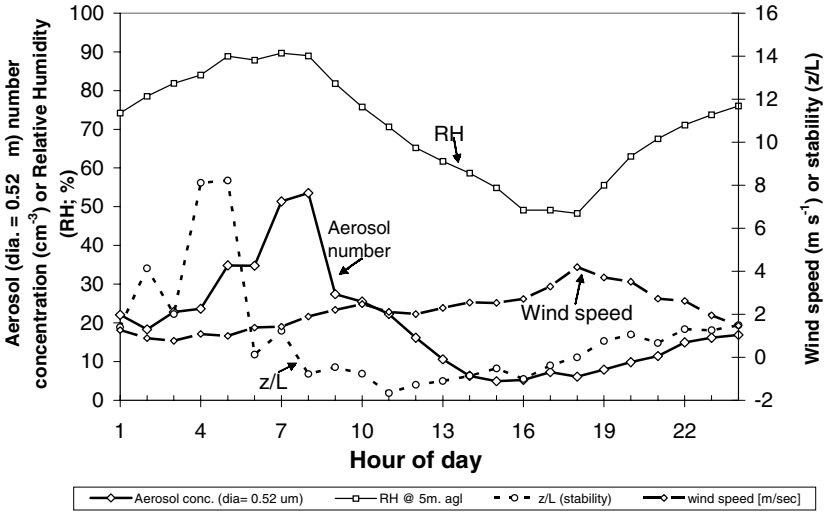

Fig. 1. Diurnal variation in winds, RH, stability and aerosol concentration during EFLAT.

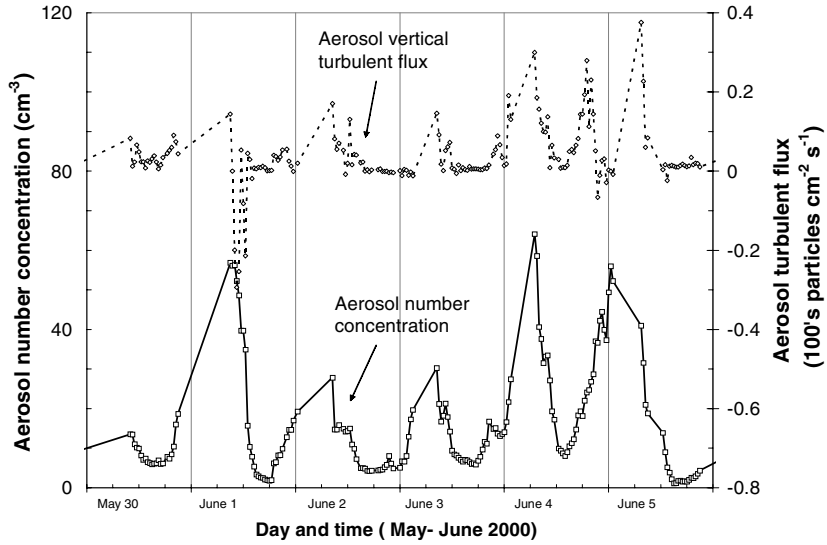

Fig. 2. Aerosol (diameter = 0.52 μm) number concentration and aerosol vertical turbulent flux measured using EC.

days. Average wind speeds, aerosol number concentrations for 0.52 μm diameter particles, relative humidity and stability (expressed as z/L where L is the Obukov length and z is 5 m; Stull, (1988)) during May and June 2000 are presented in Fig. 1.

Stable ($z/L > 0$) conditions usually occurred at night with low wind speeds ($u < 1$ m s^{-1}), high aerosol concentrations (N (diameter = 0.52 μm) > 40 cm^{-3}), and high RH (70–100%). Unstable ($z/L < 0$) conditions often occurred in the afternoon with brisk winds ($u \sim 4$ m s^{-1}), lower RH (50–60%), and lower aerosol concentrations (N (diameter = 0.52 μm) $\leq$ 10 cm^{-3}). Wind directions, although more variable, often were E to SW (pulp mills 15 to 40 km upwind) at night but W to NNW (clean, marine air upwind) during the afternoons.

4.2. *Aerosol turbulent fluxes*

Figure 2 presents nearly continuous 30-min aerosol number concentrations, N (diameter = 0.52 μm), and "uncorrected" turbulent fluxes for 6 days during June 2000. In general, the aerosol fluxes increase with aerosol concentration; subsequent presentation of aerosol turbulent fluxes as a 'deposition velocity' removes this type of scale dependence. However, the data in Fig. 2 also demonstrate that the magnitude and sign (positive fluxes are directed upwards) of the aerosol flux changes systematically near sunrise each morning during EFLAT.

The largest upward aerosol fluxes typically occurred at 7 to 8 a.m., just as solar radiation began to substantially warm the air near the surface. The transition each morning from a stable ($z/L > 0$) to an unstable (Fig. 1) boundary layer resulted in decreasing aerosol concentrations and RH. The simultaneously observed, upward aerosol fluxes are consistent with growth of the boundary layer through entrainment of cleaner air from higher altitudes. These largest upward aerosol fluxes are not descriptive of deposition to, or emission from, the vegetation surface but rather reflect the morning boundary layer growth and accompanying changes in flux with height (Businger, 1986).

Equation (4) demonstrates that surface removal of aerosol ("deposition") cannot easily be characterized by tower measurements performed during periods of flux divergence (e.g. Kowalski and Vong, 1999).

The largest observed downward (negative fluxes are directed downward) aerosol fluxes during EFLAT occurred after midnight during periods when aerosol concentration was increasing to its maximum daily value (Fig. 2). During these stable, nocturnal periods, winds were light and wind directions were generally from the South or East (i.e. the eddy flux tower was downwind of two pulp mills). An elevated, upwind emission source should produce downward turbulent aerosol flux if the advection emissions were mixed down from above the 5 m measurement height (Stull, 1988; Slinn, 1983). Downward transport of vertical velocity variance, $(w')^3$, was observed in the EFLAT data at these same time periods. These large downward fluxes occurred because advection produced a divergence in the aerosol flux.

Thus, the two major features of the aerosol turbulent fluxes that are displayed in Fig. 2 (the large downward fluxes and the large upward fluxes at 7 a.m.) are not descriptive of aerosol deposition to the vegetation surface. An analysis of surface deposition, here in terms of the aerosol deposition velocity, will necessarily require the elimination of data for the morning transition period (6 to 10 am) and for wind directions (NE, E, SE and S) that could include upwind emission sources because these data reflect periods of possible flux divergence (terms 1, 2, and 3 in eq. (4) are non-zero and probably not in balance).

4.3. *Heat and water vapour fluxes*

Heat and vapour fluxes also affect the measured EC aerosol fluxes through air density variations and particle hygroscopic growth. Figure 3 presents the EFLAT diurnally averaged EC measurements of water vapour (expressed as latent heat flux) and sensible heat (calculated from $\overline{w'T'}$) fluxes along with EFLAT measurements of net radiation, soil heat flux and the sum of sensible (SH) and latent (LH) heat fluxes. These data demonstrate that the EC measurements produce a surface energy balance where net radiation exceeds the sum of the other components by 10–20% during daytime hours; these results are typical of vegetated sites (Anthoni et al., 2000). Based on this energy balance, it appears that the vapour and heat fluxes are well characterized and appropriate for the determination of a saturation ratio flux and aerosol hygroscopic growth.

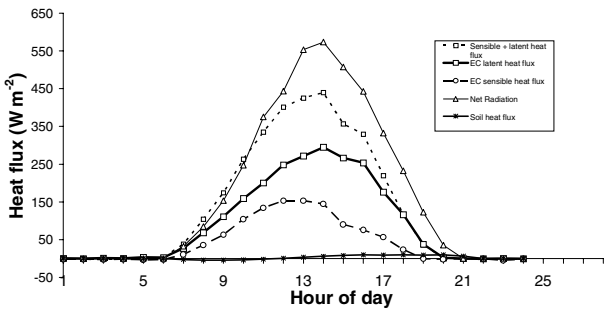

Fig. 3. Diurnal variation of measured heat fluxes during EFLAT.

4.4. *Uncertainties in flux due to particle counting and instrument separation*

An experimental set-up potentially influences the covariances (fluxes and sometimes co-spectra) due to particle counting statistics, inlet losses, slow sensor response times, physical separation of sensors and any lag time between the vertical wind and scalar measurements (Moore, 1986; Buzorius et al., 2000). Sensor response time, lag time and inlet losses were not important for the FAST during EFLAT. The ATI sonic anemometer and FAST 10 Hz response times allow the capture of most atmospheric turbulence and flux at 5 m agl (Kaimal and Finnigan, 1994). The vertical and streamwise separations of the instruments were negligible. Iso-kinetic sampling from the rotating boom minimized particle inlet losses because the instrument was pointed into the wind with the FAST's inlet face velocity equal to the wind speed (Vincent, 1989).

There are random errors ("white noise") in aerosol fluxes measured by EC due to the discrete nature of the "counts" produced by aerosol instruments such as the FAST. The minimum counting error in aerosol deposition velocity is $\sigma_w/N^{0.5}$, where N is the number of particles counted and σ_w is the standard deviation of the vertical wind velocity w for the flux time interval (Fairall, 1984; Nemitz et al., 2002; Buzorius et al., 2003). During EFLAT, the FAST particle counts typically ranged from 2×10^3 to 6×10^5 per 30 min, depending on the time of day and the particle diameter.

The noise in particle concentration due to counting is uncorrelated to vertical velocity and, thus, will affect the flux and concentration similarly (Nemitz et al., 2002). One approach to aerosol flux uncertainty due to counting noise is to compare atmospheric and counting variability. Lenschow and Kristensen (1985) introduced a "figure of merit" ($Q = 0.06(U^*/V_{dt})^2$, where U^* is friction velocity) to describe the number of particles that must be counted each second such that counting noise does not contribute significantly to the error in flux measured near the surface. For EFLAT, this figure of merit was typically 110 particles s^{-1}. Thus, counting noise usually did not significantly affect the 30-min fluxes for 0.34 and 0.52 μm diameter particles but it was an important uncertainty in the fluxes of 0.84 and 1.5 μm diameter particles.

During low-concentration periods (NW winds), the counting uncertainties for aerosol deposition velocity averaged 0.22, 0.16, 0.65 and 1.1 cm s^{-1} (Fairall, 1984; Nemitz et al., 2002) in 30-min values for particles with diameters of 0.34, 0.52, 0.84 and 1.5 μm respectively. High-concentration periods during EFLAT had counting errors that were about 25% of these values. Counting errors for the 0.34 μm diameter particles were larger than

those for the 0.52 μm diameter particles because the 0.34 μm diameter particles were undercounted by the FAST; the PCASP-calibration corrected the FAST 0.34 μm diameter aerosol concentrations but could not change the counting rate. Counting uncertainties for 30-min values of flux of the 0.84 μm diameter particles during EFLAT were of the same magnitude as V_{dt} while the 1.5 μm diameter particles had counting uncertainties that were often larger than the EC measured V_{dt}.

The counting uncertainties for pooled estimates ($N = 25$ to 38) of V_{dt} were 0.04, 0.03, 0.11 and 0.2 cm s^{-1} respectively, for 0.34, 0.52, 0.84 and 1.5 μm diameter particles. The particle counts would have been about an order of magnitude lower for most commercial instruments than these for the FAST and, thus, the counting errors would have been approximately three times larger than those obtained during EFLAT.

The EFLAT instrument lateral separation (0.51 m) influenced the EC aerosol fluxes because the aerosol and wind sensors did not always sample the same eddies. This loss of aerosol flux due to lateral separation of the sensors was investigated using EFLAT 30-min aerosol flux data and the co-spectral transfer functions proposed by Moore (1986). This approach suggests a 7% (high wind speeds) to 11% (low winds) loss of the total measured aerosol flux with nearly all of the losses predicted to occur at frequencies above 1 Hz. Losses of water vapour flux during EFLAT were smaller due to the closer placement (0.33 m) of those sensors. The final EFLAT aerosol deposition velocities (Fig. 9) were corrected for lateral separation losses.

4.5. *Spectra and co-spectra*

Another perspective on uncertainties in aerosol concentration and flux can be obtained by examining spectra and co-spectra to see how well the concentration (spectra) and flux (co-spectra) are resolved compared with turbulent timescales. Also, it is of interest to compare these turbulent transport timescales with the time required for hygroscopic growth to bring a particle to the equilibrium diameter described in eq. (3).

Figure 4 presents multi-resolution frequency spectra for temperature and the FAST aerosol concentration at four diameters. The spectrum for temperature follows the expected fall-off in normalized variance at higher frequencies (frequency >0.1, i.e. the r.h.s. of Fig. 4) at a slope of about $-5/3$, consistent with the capture of the 'inertial sub-range of atmospheric turbulence' by the sonic anemometer (Kaimal and Finnigan, 1994). Spectra for the three components of the wind velocity are similar.

The four aerosol spectra each show the influence of counting noise (such white noise produces a flattening of variance with increasing frequency) at frequencies greater than about 0.02, 0.3, 0.01 and 0.0015 s^{-1} for diameters of 0.34, 0.52, 0.84 and 1.5 μm respectively. These spectra show the importance of particle counting rate in that the particles with the highest count rate (0.52 μm diameter) are the least influenced by counting noise whereas the particles with the lowest count rate (1.5 μm diameter) appear mainly as noise in Fig. 4. For this reason, the 1.5 μm diameter aerosol will not be treated further in this analysis.

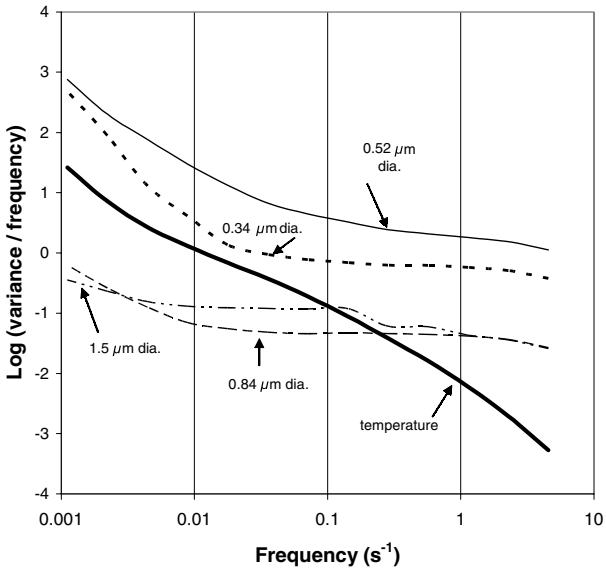

Fig. 4. Composite multi-resolution spectra for 10 Hz measurements of temperature and aerosol concentration at four particle diameters (0.34, 0.52, 0.84 and 1.5 μm).

Figure 5 presents the EFLAT multi-resolution co-spectra from the EC measurements as covariance versus frequency for the heat flux and aerosol fluxes at two diameters (without corrections for density, instrument separation or hygroscopic effects which apply to 30-min covariances). Heat fluxes are shown (Fig. 5) to occur primarily at frequencies between 0.003 and 3 s^{-1}, corresponding to timescales of 0.3 to 300 s. The EFLAT aerosol co-spectra display transport timescales that are similar to those for heat fluxes in that the turbulent fluxes of the 0.34 μm and 0.52 μm diameter particles occur at frequencies from 0.003 to 3 s^{-1} (Fig. 5). The spectrum for 0.84 μm particles is more variable, especially during unstable periods when the particle concentrations are low.

As discussed in section 4.4, uncorrelated noise in the aerosol data (Fig. 4) should not degrade the covariance data (flux) if that noise is sufficiently small (Nemitz et al., 2002). Using the approach of Lenschow and Kristensen (1985), we find that the fluxes for 0.34 and 0.52 μm diameter particles are dominated by atmospheric variability and are therefore, valid. Consistent with this finding, Fig. 5 demonstrates that the EFLAT EC system captured a substantial fraction (20–60%) of the fluxes of 0.34 and 0.52 μm diameter particles at frequencies higher than those (0.02 and 0.3 s^{-1} respectively) that correspond to the onset of counting noise (Fig. 4).

The corrections for sensor lateral separation (above) mean that the observed aerosol fluxes would be underestimated by 7–11%, with most of those losses occurring at frequencies above 1 Hz.; this damping at high frequencies is most evident in Fig. 5 for

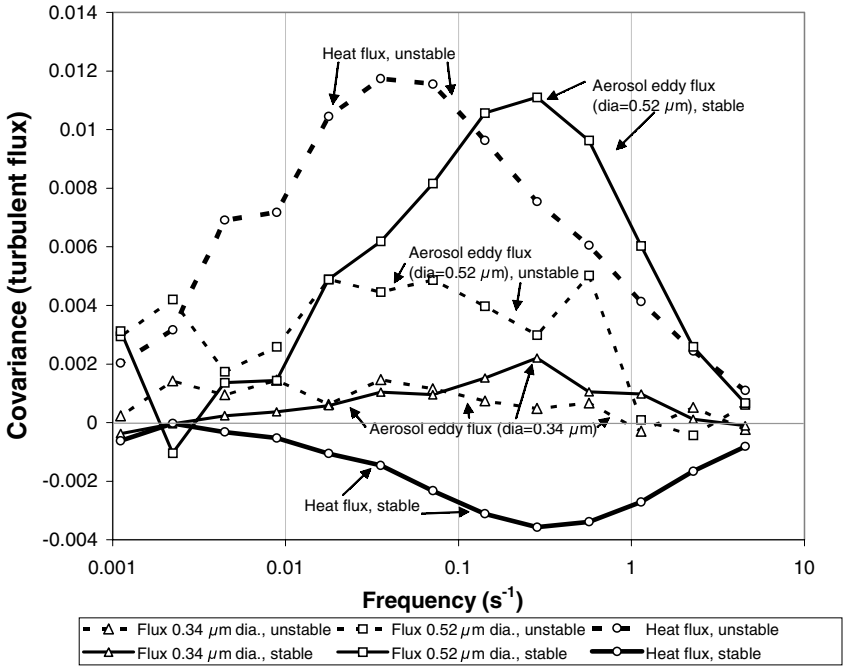

Fig. 5. Co-spectra for heat flux and aerosol fluxes at two particle diameters.

the 0.52 μm diameter particles for unstable conditions (broken curve). Thus, the lateral separation corrections (not shown) further increase the contribution of high-frequency eddies to the total aerosol flux compared with the co-spectra displayed in Fig. 5.

The spectra, co-spectra and particle counting uncertainties suggest that the best characterized EC aerosol fluxes ought to be those for 0.52 μm diameter followed by the flux of 0.34 μm diameter particles. The fluxes of 0.84 μm diameter particles have greater counting uncertainties and should be interpreted with caution. Most of the EFLAT aerosol turbulent flux occurred at timescales of about 1 to 100 s.

4.6. *Aerosol chemical composition and hygroscopic growth parameter*

Table 1 presents mean values and ranges for the aerosol chemical composition measured over 2- to 3-day periods during EFLAT, the mass ratios of each species to the sum ($NH_4 + SO_4$), and the average uncertainty in concentration (from duplicate filter collection). These data suggest that the aerosol consisted primarily of ammonium bisulfate and organic carbon compounds, with contributions from nitrate and sea salt. Very little elemental ('black') carbon was present in the air sampled during EFLAT.

Values for the aerosol hygroscopic growth factor, γ (derived by fitting eq. (3) to the data of Tang and Mucklewitz (1994), up to an RH of 96%), are presented in Table 2 as a function of solute composition and aerosol soluble volume fraction. These growth factors are valid for the aerosol size range of 0.2 to 1.0 μm.

Given an aerosol chemical composition that is dominated by NH_4, SO_4, NO_3 and organic carbon, the aerosol hygroscopic growth parameter, γ, should lie between values of 0.226 and 0.261 during EFLAT. The NH_4 to SO_4 ratio suggests a composition similar to ammonium bisulfate (increasing γ). The expected NO_3 content also supports a larger value for γ. The lack of

Table 1. Measured aerosol chemical composition (diameter <2.5 μm)

Aerosol species	Mean (μg m^{-3}) Concentration	Range (μg m^{-3})	Mass ratio to ($NH_4 + SO_4$)	Uncertainty (Δpair/mean)
SO_4	7.0	1.–18.	0.5–0.7	0.13
NH_4	4.7	0.6–8.	0.3–0.5	0.15
Na	1.4	0.2–3.	0.05–0.25	0.27
Ca	0.1	0.05–0.3	0.01–0.03	0.17
Elemental carbon	0.06	0–0.12	0–0.02	N.A.
Organic carbon	4.0	1.–10.	0.2–0.4*	N.A.
NO_3	N.A.	N.A.	0.1–0.4**	N.A.

*Based on the assumed molecular weight of carbon; total organic carbon will be larger.

**$NO_3/(NH_4 + SO_4)$ ratio is from a nearby site using the same protocol (Ko, 1992).

Table 2. Calculated hygroscopic growth parameter, γ

Aerosol composition:	$\varepsilon = 1.0$	$\varepsilon = 0.91$	$\varepsilon = 0.83$
$(NH_4)_2\ SO_4$	0.244	0.235	0.226
NH_4NO_3	0.261	0 250	0.241
$NH_4\ HSO_4$	0.261	0.250	0.241

ε = Aerosol volume fraction of the stated chemical composition (soluble fraction). The remaining aerosol volume is assumed to consist of a hygrophobic core (such as soot) that is "internally mixed".

speciation for the organic aerosol component is the major uncertainty in chemical composition pertaining to hygroscopic growth. Some of the organic carbon may be hygrophobic (decreasing γ) but the absence of elemental carbon (soot) suggests that the EFLAT aerosol was very hygroscopic. Subsequently, we use $\gamma = 0.25$ as a "best" value for calculations of the correction to the assembly average aerosol deposition velocity due to hygroscopic growth.

The variability in chemical-mass ratio rather than absolute concentration will affect our estimate of hygroscopic growth. The variability in the ratios is much smaller than the variability in concentration (Table 1). As a result of uncertainty in aerosol chemical composition we have used a range of growth factors to estimate the uncertainty in the hygroscopic growth correction to deposition velocity; the range used for γ was 0.23 to 0.255 based on the above chemical and model data and the results of Swietlicki et al. (2000). Over short (several hours) time periods the mass ratio may have been more variable than shown in Table 1. However, these periods are associated with time changes in aerosol concentration which have already been filtered from the EC data set (section 4.2). Thus, the range in γ stated above is appropriate for the calculation of the uncertainty in aerosol deposition velocity associated with hygroscopic growth.

Dry, crystalline particles will grow to 98% of their equilibrium diameter (diameter at 98% RH) over timescales of 65, 163 and 400 ms for particle diameters of 0.25, 0.4 and 0.63 μm respectively (Keith and Arons, 1954). During EFLAT the maximum short-term variation in ambient relative humidity at the EC measurement height was no more than 5–7% such that the timescale for hygroscopic growth (tens of milliseconds) was much less than the timescale for vertical transport (tens of seconds) by turbulent eddies; this supports the use of an equilibrium model for hygroscopic growth of sub-μm diameter particles.

Future EC experiments would benefit from direct measurement of the size distribution at multiple humidities or the hygroscopic growth factor at several sizes and humidities within the range of interest.

4.7. *Hygroscopic growth correction to aerosol deposition velocity*

During EFLAT relatively dry air advected over wet and transpiring grass setting up a vertical gradient in RH. For a given aerosol dry size, the ambient aerosol diameter was smaller in air aloft than it was for more humid air near the surface. Thus, upward-moving aerosol contained more liquid water than downward-moving aerosol; this extra water in upward moving particles usually produced an apparent (false) upward flux of aerosol in the 'uncorrected' EC data for all particles sizes.

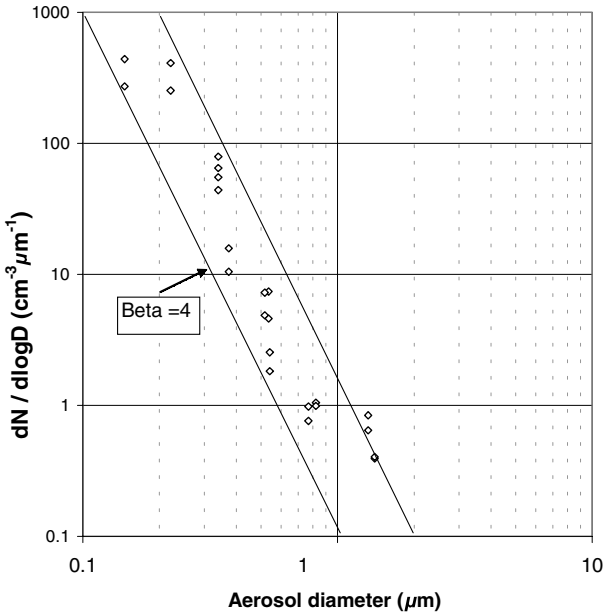

Fig. 6. Aerosol size distribution from EFLAT from three instruments for consecutive 30-min periods from 3–4 p.m. on 8 June 2000. A constant slope (β) of 4 is illustrated (β) for comparison only. Separate values of β for each diameter (Table 3) were calculated every 30 min from measurements for use in the hygroscopic growth correction (eq. (8)).

Figure 6 presents the aerosol number size distribution for consecutive 30-min periods during the afternoon of 8 June 2000. Multiple aerosol instruments were used to determine the best values for β for each 30-min period; typical values of β are presented in Table 3 for each diameter at which eddy fluxes were determined from the FAST. The large abundance of smaller particles ($\beta > 0$) that occurred throughout EFLAT is evident in Fig. 6, as is the 30-min variability in number concentration. These local values of β provide the best estimate of the number of smaller particles that can grow into a specific size interval due to increases in RH.

The aerosol deposition velocities for the "best characterized" particle size (0.52 μm diameter) are presented in Fig. 7 as the "corrected-measured" V_{dt} (for values of γ of 0.235, 0.25 and 0.255). Figure 7 also presents the EC measurements and the "apparent deposition velocity due to hygroscopic growth" for $\gamma = 0.25$, i.e. $-\Delta V_{dt}$ (as a dashed line). Whereas the measured values for V_{dt} and the values of $-\Delta V_{dt}$ were typically positive (upwards), the "corrected-measured" V_{dt} are negative (downward). The hygroscopic growth correction during EFLAT was

Table 3. Slope of the aerosol size distribution, β

EC flux, diameter interval (median diameter)	Geometric mean diameter used for β	Instruments for β	Range for β
0.31–0.375 μm (0.34 μm)	0.22, 0.34 μm	HSLAS	3.0 to 5.2
0.375–0.716 μm (0.52 μm)	0.34, 0.54, 0.77 μm	LASX, HSLAS	3.3 to 5.5
0.716–0.98 μm (0.84 μm)	0.54, 0.77, 0.84 μm	FAST,LASX,HSLAS	3.2 to 6.0
0.98–2.3 μm (1.5 μm)	0.82, 1.4, 1.5 μm	FAST,LASX	1.1 to 2.7

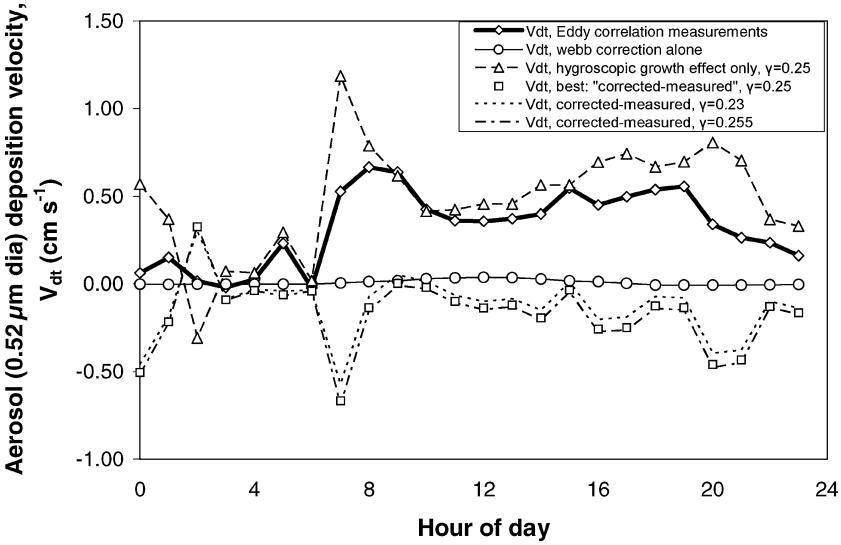

Fig. 7. Aerosol deposition velocity (diameter = 0.52 μm) is presented for the EC measurements, hygroscopic growth correction, Webb correction and fully corrected values (for $\gamma = 0.235$, 0.25 and 0.255).

typically between 0.2 and 0.7 cm s^{-1} (depending on the hour of the day) with an uncertainty of $\pm$ 0.03–0.06 cm s^{-1} due to uncertainty in γ associated with chemical composition. EFLAT aerosol deposition velocities are not very sensitive (change in $\Delta V_{\rm dt} \leq 10\%$) to the choice of the hygroscopic growth parameter within the expected range ($0.235 \leq \gamma \leq 0.255$).

Figure 8 presents the measured values of saturation ratio (S), saturation ratio flux ($\overline{w'S'}$), and the slope of the aerosol size distribution (β at 0.52 μm diameter) that were used to calculate the hygroscopic growth correction ($\Delta V_{\rm dt}$). During EFLAT, the saturation ratio flux exhibited large diurnal variations with low values at night but large values during afternoons. Values of β derived from each of the three aerosol instruments exhibited a marked diurnal variation with minimum values at night and maximum values during the afternoon. Afternoon measurements of $\overline{w'S'}$ during EFLAT fell between previously reported values taken for forests located in Canada and Finland (Buzorius et al., 2000; Kowalski, 2001).

The diurnal variations in β and $\overline{w'S'}$ during EFLAT means that there are relatively more of the smaller particles (β large) available for hygroscopic growth into a given diameter interval and that they will experience larger RH increases ($\overline{w'S'}$ large) in the afternoon than at night. Thus, the magnitude of the hygroscopic growth correction in the afternoon is large compared with values for morning or night-time periods during EFLAT. The correction to aerosol turbulent flux ($\Delta V_{\rm dt}$) most

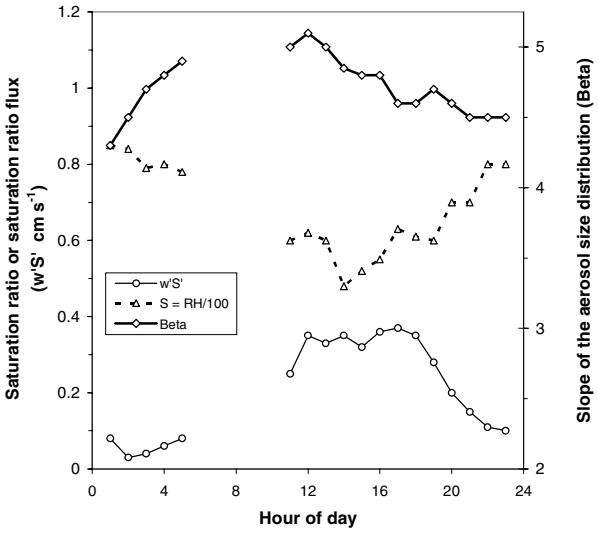

Fig. 8. Components of the hygroscopic growth correction during EFLAT. Hourly averages of measured values of saturation ratio (S), saturation ratio flux ($\overline{w'S'}$), and the slope of the aerosol (diameter = 0.52 μm) size distribution (β) are shown for the time periods that are used in Fig. 9.

closely tracks the diurnal variation in saturation ratio flux (Figs. 7 and 8).

The calculated hygroscopic growth correction for 0.34 and 0.84 μm diameter particles was similar to that for 0.52 μm

diameter particles because ΔV_{dt} varies between particle sizes only due to variation in the slope of the size distribution (β). Aerosol chemical composition was not sufficiently size resolved from EFLAT filter measurements to determine different values of γ for different particle diameters even though this composition is known to be size dependent. Thus, the size dependence of γ, ΔV_{dt}, and the "measured-corrected" aerosol deposition velocities are not as well characterized as are their average values within the accumulation mode diameter interval (0.3–1 μm here). Other uncertainties in the size dependence of ΔV_{dt} result from the fact that 0.84 μm diameter particles are 2.6 times slower to reach their equilibrium size than are the 0.52 μm diameter particles ($\sim d^2$ dependence of growth rate; Keith and Arons, 1954). Thus, it is possible that eqs. (3) and (8) overestimate hygroscopic growth for the largest aerosol (0.84 μm diameter) considered here (Zufall et al., 1998) although Fairall (1984) suggests that these particles will reach equilibrium with ambient RH during turbulent transport and mixing.

The Webb, or density, correction to aerosol flux during EFLAT is much smaller than the hygroscopic growth correction, reaching a maximum of 0.05 cm s^{-1} during the afternoon (circles on Fig. 7). The major impact of heat and vapour fluxes on aerosol deposition velocity corrections is through hygroscopic growth rather than the Webb correction.

The deposition velocities in Fig. 7 represent hourly averaged values with RH <96% that passed a quality assurance screening criterion; they have not been screened for either wind direction or the morning transition period and, therefore, cannot be considered to represent "deposition to the grass surface". Examples of data that do not represent surface deposition are (a) the upward V_{dt} that are typical at 2 a.m. (increasing aerosol concentration and, probably, maximum advection from pulp mills that are upwind during that time of day) and (b) the large downward V_{dt} that occur around 7 a.m. (start of the morning transition period when boundary layer growth and flux divergence are occurring). Such data are not included in the final EFLAT results (Fig. 9).

4.8. *Aerosol deposition velocity as a function of stability*

Figure 9 presents the EFLAT data that best describe aerosol deposition to the grass surface, i.e. those that are least likely to have been sampled during periods of vertical flux divergence. Corrected aerosol deposition velocity for three particle sizes are summarized for a total of 86 30-min measurement periods with the very best fetch (NW winds) while avoiding the morning transition period. Given that there are no obvious aerosol sources to the NW, this data stratification minimizes any influence of advection.

Figure 9 demonstrates the expected relationship (Lamaud et al., 1994) between deposition velocity (V_{dt}) and stability (as *z/L)* in that unstable periods display larger downward (more negative) V_{dt} than do neutral or stable periods during EFLAT. As

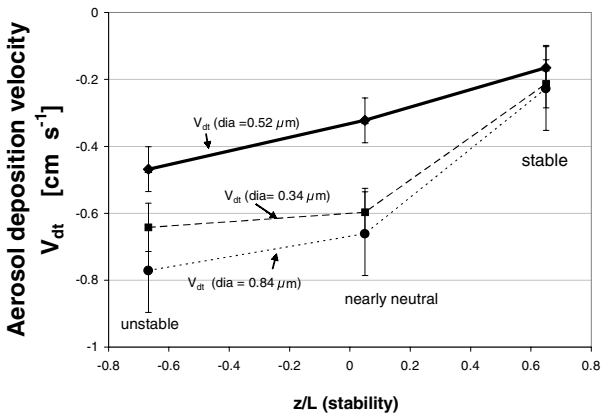

Fig. 9. Aerosol deposition velocity varies with stability (*z/L*). Eddy correlation field data have been corrected for hygroscopic growth (γ = 0.25), sensor lateral separation and density (Webb correction). Pooled uncertainties (counting and hygroscopic growth) are indicated for each particle diameter.

conditions changed from stable to unstable, the aerosol deposition velocity for 0.52 μm diameter particles increased from 0.16 to about 0.44 cm s^{-1} while V_{dt} for 0.34 and 0.84 μm diameter particles increased from 0.2 to 0.6 and 0.7 cm s^{-1} respectively. The increased deposition velocity with unstable conditions is expected because turbulent transport through the atmospheric surface layer increases and surface impaction of transported particles is likely to be more efficient with the higher wind speeds that occur.

The consideration of counting and hygroscopic growth uncertainties together (assuming that these uncertainties are independent, e.g. Duan et al., 1988) leads to overall (pooled) uncertainties in deposition velocity of 0.072, 0.067 and 0.125 cm s^{-1} for particle diameters of 0.34, 0.52 and 0.84 μm respectively (displayed as errors bars in Fig. 9).

Since the 0.52 μm diameter particles were typical of the aerosol collected for chemical composition, were counted at 100% efficiency, had the smallest counting uncertainties and have short equilibrium times for hygroscopic growth, we consider these 0.52 μm diameter values for V_{dt} to be the most reliable. Differences in the values for V_{dt} for 0.34 and 0.84 μm diameter particles (Fig. 9) are not significant given the uncertainties associated with hygroscopic growth and counting statistics.

The EFLAT 0.52 μm diameter value of 0.44 cm s^{-1} for V_{dt} during unstable conditions is a little larger than values reported by Wesely et al. (1983, 1985) while the EFLAT value of 0.3 cm s^{-1} during near-neutral conditions is similar to experimental values reported by Hummelshoj (1994), Gallagher et al. (1997), and Nemitz et al. (2002) for particles of this size.

5. Summary and conclusions

Eddy correlation measurements of aerosol fluxes were performed with a new high-flow-rate aerosol spectrometer at a site

that was ideal for determining deposition during selected time periods. The high flow rates of the FAST spectrometer reduced uncertainties in the flux by increasing the number of particles counted. Data were selected to avoid vertical divergence in the flux due to advection of upwind source emissions and boundary layer growth.

The FAST measured aerosol size at ambient RH; this produced aerosol turbulent fluxes that were biased "upwards" due to vertical changes in RH and particle hygroscopic growth. This effect was quantified by an analysis based on separate measurements of aerosol composition, aerosol size distribution, RH and saturation ratio flux and was removed from the EC field measurements to produce estimates of the "true value" of aerosol deposition velocity to the grass surface for three particle sizes.

Other studies of aerosol deposition velocity could also have a bias towards upwards fluxes if based on aerosol diameter that is measured at, or near, ambient RH. Studies that dry the aerosol (to RH $< 30\%$) before sensing (Gallagher et al., 1997) ought to avoid this bias and any need for a hygroscopic growth correction. The hygroscopic growth correction to the aerosol flux was large in this study because the aerosol was composed of very hygroscopic compounds, the aerosol size distribution was 'steep' (there were lots of small particles to grow with increasing RH) and the vertical changes in RH were relatively large due to the presence of wet soils underlying dry air. Future studies might focus on improving estimates of the hygroscopic growth factor (γ) in order to reduce uncertainties in the hygroscopic growth correction (ΔV_{dt}) related to the presence of organic or hygrophobic compounds and their size dependence; real-time values of γ could be obtained using tandem differential mobility analyses (Swietlicki et al., 2000). For the current study, the corrected deposition velocities for 0.52 μm diameter particles have an estimated pooled uncertainty of ± 0.07 cm s^{-1} due to chemical composition (choice of γ) and counting statistics.

For the best characterized particles (0.52 μm diameter) during EFLAT, the measured and fully corrected aerosol deposition velocity to grass was 0.16 cm s^{-1} during stable conditions, 0.3 cm s^{-1} in near neutral conditions and 0.44 cm s^{-1} during unstable conditions.

6. Acknowledgments

The authors thank Siddharth Pavithran and Darren O'Connor for software development, Rondi Robeson and Marcus Appy for field measurements, Greg Kok for the PCASP-FAST comparison, and George Pugh for the use of his grass seed field. This project was supported by NSF grant no. 9907765-ATM (Atmospheric Chemistry).

7. Appendix A

Using the Swietlicki et al. (2000) hygroscopic growth relationship, the dependence of aerosol equilibrium diameter on saturation ratio S, i.e. RH/100, is

$$\mathrm{d}D/\mathrm{d}S = D\gamma/(1 - S).$$

If aerosol size and number are measured at ambient RH, an error occurs in the corresponding aerosol turbulent flux within the specified size interval when that flux is measured by EC. This error occurs for two reasons:

(a) more particles typically grow into a size interval (for $\beta >$ 0) than out of it when the RH increases;.

(b) the dry particle diameters that correspond to the limits of the size interval change with RH because the interval is defined in terms of diameter at ambient RH.

These two effects can be expressed (Fairall, 1984; Kowalski, 2001) as:

$$\mathcal{N}' = D'(\mathrm{d}\mathcal{N}/\mathrm{d}D + \mathcal{N}/D)$$

where $\mathcal{N}'$ is the increase in aerosol number concentration spectral density (at a given mean diameter) that is associated with hygroscopic growth during vertical transport.

Introducing the Junge power law to relate the number of particles of different diameters one obtains

$$\mathcal{N}'/\mathcal{N} = -\beta(D'/D).$$

Combining this with the definition of deposition velocity and the change in aerosol size at equilibrium for a perturbation (S') in saturation ratio ($D' = S'\,\mathrm{d}D/\,\mathrm{d}S$), the change in the aerosol deposition velocity due to hygroscopic growth is thus

$$\Delta V_{\mathrm{dt}} = w'\mathcal{N}'/\mathcal{N} = -\beta w' D'/D = -\beta(\overline{w'S'}/D)(\mathrm{d}D/\mathrm{d}S)$$

or

$$\Delta V_{\mathrm{dt}} = -\beta\gamma\overline{w'S'}/(1 - S).$$

References

Anthoni, P. M., Law, B. E., Unsworth, M. H. and Vong, R. J. 2000. Variation in net radiation over heterogeneous surfaces: measurements and simulation in a juniper-sagebrush ecosystem. *Agric. Forest Meteor.* **102**, 275–286.

Birch, M. and Cary, R. 1996. A thermal-optical technique for analysis of aerosol carbon compounds. *Aerosol Sci. Technol.* **25**, 221–241.

Businger, J. A. 1986. Evaluation of the accuracy with which dry deposition can be measured with current micrometeorological techniques. *J. Climate Appl. Meteorol.* **25**, 1100–1124.

Buzorius, G., Rannik, U., Makela, J. M., Keronen, P., Vesala, T. and Kulmala, M. 2000. Vertical fluxes measured by the eddy correlation method and deposition of nucleation mode particles above a Scots pine forest in southern Finland. *J. Geophys. Res.* **105**, 19 905–19 916.

Buzorius, G., Rannik, U., Nilsson, E. D., Vesala, T. and Kulmala, M. 2003. Analysis of measurement techniques to determine dry deposition velocities of aerosol particles with diameters less than 100 nm. *J. Aerosol Sci.* **34**, 747–764.

Duan, B., Fairall, C. W. and Thomson, W. 1988. Eddy correlation measurements of the dry deposition of particles in the wintertime. *J. Appl. Meteorol.* **27**, 642–652.

Fairall, C. W., 1984. Interpretation of eddy correlation measurements of particulate deposition and aerosol flux. *Atmos. Environ.* **18**, 1329–1337.

Gallagher, M. W., Beswick, K. M., Duyzer, J., Westrate, H., Choularton, T. W. and Hummelshoj, P. 1997. Measurements of aerosol fluxes to Speulder Forest using a micrometeorological technique. *Atmos. Environ.* **31**, 359–373.

Hummelshoj, P. 1994. Dry deposition of particles and gases, *RISO National Laboratory Report RISO-R-658(EN)*, RISO National Laboratory, Roskilde, Denmark.

Junge, C. E. 1963. *Air Chemistry and Radioactivity.*, **Vol. 4**, Academic Press, New York, 114–123.

Kaimal, J. C. and Finnigan, J. J. 1994. *Atmospheric Boundary Layer Flows: their Structure and Measurement.* Oxford University Press, New York, 33–39.

Keith, C. H. and Arons, A. B. 1954. The growth of seasalt aerosol particles by condensation of atmospheric water vapor. *J. Meteorol.* **11**, 173–184.

Ko, L.-J. 1992. *Factors influencing the atmospheric aerosol composition at two sites in western Oregon.* M.S. Thesis, Oregon State University, USA.

Kowalski, A. S. 2001. Deliquescence induces eddy covariance and estimable dry deposition errors. *Atmos. Environ.* **35**, 4843–4851.

Kowalski, A. S. and Vong, R. J., 1999. Near-surface fluxes of cloud water evolve vertically. *Q. J. R. Meteorol. Soc.* **125**, 2663–2684.

Kowalski, A. S., Anthoni, P. M., Vong, R. J., Delany, A. C. and Maclean, G. D. 1997. Deployment and evaluation of a system for ground-based measurement of cloud water turbulent fluxes. *J. Atmos. Ocean Technol.* **14**, 468–479.

Lamaud, E., Brunet, Y., Labatut, A., Lopez, A., Fontan, J. and Druilhet, A., 1994. The Landes experiment: biosphere-atmosphere exchanges of ozone and aerosol particles above a pine forest. *J. Geophys. Res.* **99**, D8, 16 511–16 521.

Lenschow, D. H. and Kristensen, L. 1985. Uncorrelated noise in turbulence measurements. *J. Atmos. Ocean Technol.* **2**, 68–81.

Moore, C. J., 1986. Frequency response corrections for eddy correlation systems. *Bound. Layer Meteorol.* **37**, 17–35.

Nemitz, E., Gallagher, M. W., Duyzer, J. H. and Fowler, D. 2002. Micrometeorological measurements of particle deposition velocities to moorland vegetation. *Q. J. R. Meteorol. Soc.* **128**, 2281–2300.

Slinn, W. G. N. 1983. A potpourri of deposition and resuspension questions. In: *Precipitation Scavenging, Dry Deposition, and Resuspension*, Volume 2, (eds Pruppacher, H. R., Semonin, R. G. and Slinn, W. G. N.) Elsevier Scientific, New York, 1361–1416.

Stull, R. B. 1988. *An introduction to boundary layer meteorology.* Kluwer Academic, Dordrecht, 90–92.

Swietlicki, E., Zhou, J. Covert, D. S., Hameri, K., Busch, B. and coauthors, 2000. Hygroscopic properties of aerosol particles in the northeastern Atlantic during ACE-2. *Tellus* **52B**, 201–227.

Tang, I. N. and Mucklewitz, H. R., 1994. Water activities, densities, and refractive indices of aqueous sulfates and sodium nitrate droplets of atmospheric importance. *J. Geophys. Res.*, **99** D9, 18 801–18 808.

Vickers, D. and Mahrt, L. 1997. Quality control and flux sampling problems for tower and aircraft data *J. Atmos. Ocean. Technol.* **14**, 512–526.

Vickers, D. and Mahrt, L. 2003. The cospectral gap and turbulent flux calculations. *J. Atmos. Ocean. Technol.*, **20**, 660–672.

Vincent, J. H. 1989. *Aerosol Sampling, Science and Practice*, John Wiley, New York, 86–118.

Vong, R. J. and Kowalski, A. S., 1995. Eddy correlation measurements of size-dependent cloud droplet turbulent fluxes to complex terrain, *Tellus* **47B**, 331–352.

Webb, E. K., Pearman, G. I. and Leuning, R. 1980. Correction of flux measurements for density effects due to heat and water vapor transfer. *Q. J. R. Meteorol. Soc.* **106**, 85–100.

Wesely, M. L., Cook, D. R. and Hart, R. L. 1983. Fluxes of gases and particles above a deciduous forest in wintertime. *Bound. Layer Meteorol.* **27**, 237–255.

Wesely, M. L., Cook, D. R. and Hart, R. L. 1985. Measurements and parameterization of particulate sulfur dry deposition over grass. *J. Geophys. Res.* **90**, 2131–2143.

Zufall, M. J., Bergin, M. H. and Davidson, C. I. 1998. Effects of non-equilibrium growth of ammonium sulfate on dry deposition to water surfaces. *Environ. Sci. Technol.* **32**, 584–590.